A two-ejecta event associated with a two-step geomagnetic storm

C. J. Farrugia,[1] V. K. Jordanova,[1,2] M. F. Thomsen,[2] G. Lu,[3] S. W. H. Cowley,[4] and K. W. Ogilvie[5]

[1]   A new view on how large disturbances in the magnetosphere may be prolonged and intensified further emerges from a recently discovered interplanetary process: the collision/merger of interplanetary (IP) coronal mass ejections (ICMEs; ejecta) within 1 AU. As shown in a recent pilot study, the merging process changes IP parameters dramatically with respect to values in isolated ejecta. The resulting geoeffects of the coalesced ("complex") ejecta reflect a superposition of IP triggers which may result in, for example, two-step, major geomagnetic storms. In a case study, we isolate the effects on ring current enhancement when two coalescing ejecta reached Earth on 31 March 2001. The magnetosphere "senses" the presence of the two ejecta and responds with a reactivation of the ring current soon after it started to recover from the passage of the first ejection, giving rise to a double-dip (DD) great storm (each min $Dst < -250$ nT). A drift-loss global kinetic model of ring current buildup shows that in this case the major factor determining the intensity of the storm activity is the very high (up to ~ 10 cm^{-3}) plasma sheet density. The plasma sheet density, in turn, is found to correlate well with the very high solar wind density, suggesting the compression of the leading ejecta as the source of the hot, superdense plasma sheet in this case. This correlation is similar to that obtained in a previous investigation extending over several years, but the present case study extends the range of plasma sheet densities from ~ 2 to ~ 10 cm^{-3}. Since the features of the ejecta interaction in this example are fairly general, we propose that interacting ejecta are a new, important IP source of DD major storms. Peculiarities in the behavior of the magnetopause current during these extreme events are briefly discussed in the light of recent work. In a brief discussion of a second example (21–23 October 2001), we suggest that by strengthening the leading shock, the ejecta merger may have added to the "shock-driver gas" origin of DD geomagnetic storms by increasing the ability of the shock to compress preexisting $B_z < 0$ magnetic fields.

1. Introduction

[2]   By now, the disruptive potential of ejecta and the subset thereof, magnetic clouds, has been amply documented [see, e.g., *Zhang and Burlaga*, 1987; *Gonzalez and Tsurutani*, 1987; *Tsurutani et al.*, 1988, 1992; *Gosling*, 1993; *Gosling et al.*, 1990, 1991; *Farrugia et al.*, 1993a, 1993b, 1993c, 1998; *Freeman et al.*, 1993; *Gosling*, 1990; *Farrugia et al.*, 1997]. During such disturbed conditions, aurorae are excited, even down to unusually low latitudes, the ring current is enhanced, sometimes producing "great" storms ($Dst < -250$ nT), a periodic sequence of substorms may occur during the continued forcing [*Farrugia et al.*, 1993a; *Huang et al.*, 2003a, 2003b]; power is deposited in the ionosphere in the 100s of GW range, and so forth. These are some of the reasons why ejecta and magnetic clouds and their inner heliospheric propagation feature so prominently in all discussions of space weather.

[3]   Let us focus for the moment on magnetic clouds, i.e., large mesoscale (fraction of an AU), low-beta magnetoplasmas in which a strong magnetic field rotates smoothly over a large angle [*Burlaga et al.*, 1981]. During their ~ 1 day passage at Earth, the magnetosphere is typically embedded for a long period (many hours) in strong and southward magnetic fields followed/preceded by a period of northward field. Broadly similar conditions occur when other interplanetary manifestations of coronal mass ejections (ICMEs, called henceforth "ejecta") pass Earth. Thus

[1] Space Science Center and Physics Department, University of New Hampshire, Durham, New Hampshire, USA.
[2] Los Alamos National Laboratory, Los Alamos, New Mexico, USA.
[3] High Altitude Observatory, National Center for Atmospheric Research, Boulder, Colorado, USA.
[4] Department of Physics and Astronomy, University of Leicester, Leicester, UK.
[5] NASA Goddard Space Flight Center, Greenbelt, Maryland, USA.

the standard view on ejecta-driven storms, and the majority of major storms (i.e., $Dst < 100$ nT) fall into this category, is that the main phase of the geomagnetic storm coincides in time with the southward pointing ejecta phase, which is then followed by a long recovery when the field turns north again or the ejecta passage ends. Storm experts call the corresponding Dst profile a one-step storm, i.e., one with a single Dst minimum, caused by a single IP trigger (i.e., the long phase of $B_z < 0$).

[4] This paradigmatic thinking may, however, need to be revised if we want to have a proper understanding of solar wind coupling during very large disturbances. A major critique of the paradigm comes from storm specialists. Thus in a statistical study of over 1200 storms spread over 3 solar cycles, *Kamide et al.* [1998] found that the majority (67%) of intense storms ($Dst < -100$ nT) were in fact two-step storms in which, after the first Dst minimum is reached, a brief (few hours) partial recovery intervenes, to be followed by another Dst minimum. While the majority of two-step storms were such that the first Dst minimum was weaker than the second, there were $\sim 8.5\%$ where the reverse was the case. In view of this surprising finding, Kamide et al. suggested that "our future efforts should be directed toward identifying the cause for a two-stage structure in the southward IMF, not one large southward turning." Importantly, they also argued that intense magnetic storms may result from a superposition effect, rather than from a single, intense disturbance in the IMF (see also review by *Daglis et al.* [2003]).

[5] What might be the IP source of these frequent two-step storms? A possibility, very popular with the community, is that we are dealing with the successive contributions to ring current (RC) buildup from, first, the shock ahead of the ejecta (where the shock has intensified an already southward oriented IMF) and, second, to the southward field in the ejecta proper [*Gonzalez et al.*, 1989; *Gosling et al.*, 1990, 1991; *Tsurutani et al.*, 1988, 1992]. Indeed, this mechanism is certainly responsible for many two-step storms.

[6] It is our purpose here to argue that this is, however, not the whole answer; ejecta mergers (see below) may provide another source, perhaps even more important than the "shock-driver gas" configuration in the sense of producing the largest two-step storms. The sources of the geoeffects are then twofold: the parameters of the individual, noninteracting ejecta themselves, and their further enhancement through the merging process.

[7] In a remarkable recent discovery, *Gopalswamy et al.* [2001, 2002] gave an example of coronal mass ejections released in rapid succession and colliding near the Sun, as signalled by a burst of broadband radio emissions. In the ensuing collision, the leading ejecta was accelerated and diverted from its original path, as observed by SOHO/LASCO. At about the same time, *Burlaga et al.* [2001] studied fast ejecta (i.e., passing Earth with a speed >600 km s^{-1}) over a 650-day period during the rising phase of this solar cycle (1998–1999). These structures were of two types: some had the configuration of magnetic clouds [*Burlaga et al.*, 1981, 1990], while others had a disordered field but contained many acknowledged signatures of ejecta (elevated He^{++}/H^+ density ratios, strong fields, low proton beta, counterstreaming suprathermal electrons, unusual

composition, Forbush decreases, and so forth [e.g., *Zwickl et al.*, 1983; *Gosling et al.*, 1987; *Richardson and Cane*, 1995; *Neugebauer and Goldstein*, 1997; *Cane and Richardson*, 2003]. This latter category were labelled "complex ejecta." Their compositional and other properties led Burlaga et al. to suggest that complex ejecta might have been formed when several CMEs coalesced. Even so, at 1 AU they presented a simple bulk speed profile characteristic of a single stream. Significantly, while roughly equal numbers of magnetic clouds and complex ejecta were identified in their sample, the duration of Earth passage of the latter was about three times as long (~ 3.1 versus 1 day). This carries the implication that the Earth would be immersed in unusual IP conditions for a much longer time. In addition, these events are not uncommon [see also *Farrugia et al.*, 2006].

[8] In a subsequent work, *Burlaga et al.* [2002] pursued this line of thought further and gave examples of successive CMEs released at the Sun and corresponding complex ejecta at 1 AU. The presence of various shocks hinted that the merger was not complete (since merging involves the transfer of the momentum of the shock-sheath from one ejecta to the other [*Farrugia and Berdichevsky*, 2004]). All examples were associated with major and prolonged disturbances at Earth, as gauged by the storm time Dst index.

[9] In this paper we take a specific example of an ejecta-ejecta interaction and show it to be a dominant source of a two-step great (uncorrected $Dst < -250$ nT) storm. Discussing what specific IP processes are responsible for the extreme severity of the storm (in temporal order, the minimum Dst not corrected for magnetopause currents is -370 and -280 nT), we find that a key factor is the elevated density in the plasma sheet (up to 10 cm^{-3} with an average of 5 cm^{-3}). We show that this density, and its temporal profile, are correlated with the solar wind density, which, in turn, we suggest to be the result of the compression of the plasma in the leading ejecta.

[10] We then present a second example, also one involving interacting ejecta, where the DD storm (with the first peak stronger than the second) was due to the conventional mechanism. We argue plausibly that the severity of the first storm phase was due in part to the ejecta interaction. Specifically, this interaction is likely to have strengthened the leading shock and hence increased its efficiency for compressing $B_z < 0$ fields upstream of it.

2. Near-Earth Signatures Ejecta-Ejecta Interactions

[11] Studying two 1-month intervals separated by two solar cycles and in the same phase of the cycle (April 1979, 2001), *Berdichevsky et al.* [2003] and *Farrugia and Berdichevsky* [2004] found the following IP signatures of two interacting ejecta. There was (1) a strengthening of the leading shock; (2) a weakening of the shock formerly driven by the trailing ejecta or its merger with the leading shock; (3) the transfer of the momentum of the shock and its postshock flow to the leading ejecta; (4) acceleration/deceleration of the leading/trailing ejecta through momentum transfer; (5) compression of the magnetic field and plasma of the leading ejecta; and (6) heating of the plasma. Many of these signatures were also obtained in the 2 1/2-dimensional MHD numerical simulations of the interaction of magnetic

flux ropes by *Odstrcil et al.* [2003]. Specializing to the compression and heating of the plasma, we may cite the recent simulations undertaken by *Lugaz et al.* [2005] who used a three-dimensional (3-D), compressible MHD code to study aspects of ejecta mergers, and compared their findings to the main event (31 March 2001) we are studying. Their flux ropes are taken from the category of *Gibson and Low* [1998] and consist of closed field lines rooted at the Sun. They find considerable compression and heating of the plasma, which they attribute mainly to the passage through the leading ejecta of the trailing shock. The simulations reproduce the main features of the observations well (see their Figure 9).

[12] Much past work would suggest that these effects would tend to intensify the geoeffects of the separate ejecta. The implication is that the geoeffects of ejecta-ejecta interactions are due to a superposition of sources. There are first the effects which would be elicited by the individual ejecta. On top of these there are the intensifications thereof stemming from the interaction.

3. Interplanetary Observations on 31 March 2001

[13] Plasma and magnetic field observations made by the Wind spacecraft [*Ogilvie et al.*, 1995] for the period 0000 UT, 31 March, to 0400 UT, 1 April, are shown in Figure 1. The data are from the MFI [*Lepping et al.*, 1995] and 3-D Plasma Analyzer [*Lin et al.*, 1995] instruments, respectively. The time resolutions of the data in Figure 1 are 3 s (plasma) and 90 s (magnetic field). From top to bottom the panels show the total (proton plus α particles) density, proton bulk speed and temperature, total dynamic pressure (black) and proton beta (blue trace; scale on the right), the solar wind electric field (calculated as $V_x\sqrt{\left(B_y^2 + B_z^2\right)}$), the GSM components of the magnetic field, and the total field strength. The red trace in the temperature panel gives expected solar wind temperatures from statistical analyses [*Lopez*, 1987], and it may be noted that it gives comparable values to those measured, due to the plasma heating during the interaction.

[14] Wind was executing the first of four distant prograde orbits, and during the interval of interest it was situated at $(0, -255, 5)$ R_e (GSE coordinates). For the normal solar wind, at these distances coherence with near-Earth solar wind and IMF parameters would typically be lost [*Crooker et al.*, 1982; *Richardson and Paularena*, 2001]. However, ejecta coherence lengths are much longer in both X [*Farrugia et al.*, 2005a] and Y [*Farrugia et al.*, 2005b] directions. Cross-correlating the magnetic field and plasma parameters measured by ACE and Wind in the period of ejecta 1 and 2 marked in Figure 1, we find cross-correlation coefficients of 0.7 for B_x, B_y, B, density and bulk speed, and 0.9 for B_z. We shall thus use Wind data in the following.

[15] Comparing the arrival times of the shock at Wind (marked "S") and the sudden impulse signature in low latitude ground magnetograms, we find no significant delay. We shall thus assume insignificant propagation delay of IP features from Wind to the magnetosphere.

[16] By comparing the in situ data at 1 AU with solar observations, two fast ejecta were identified in the period

shown in Figure 1 [*Berdichevsky et al.*, 2003; *Wang et al.*, 2003; *Farrugia and Berdichevsky*, 2004], as marked in the bottom panel. They extend from 0600 to 2200 UT, where the end time of the second ejecta, which is uncertain, is plotted as coinciding with the arrival of the leading edge of a fast stream at 2200 UT.

[17] Various concurrent disturbances (in particular an excursion to $\beta > 1$ values at $\sim$1230–1400 UT), mark the vestige of a boundary [*Farrugia and Berdichevsky*, 2004]. A shock is present ahead of the ejecta merger, whose time of arrival is indicated by first vertical guideline. A weak shock/wave front is advancing into the trailing ejecta (second vertical guideline). We emphasize that this disturbance plays no further role in what follows.

[18] The general trend for the density is to decrease from peak value >100 cm^{-3} to values of order 4 cm^{-3}. Compression of plasma in the leading ejecta is one of the features of these ejecta mergers/partial mergers and plays a key role in what follows. One of the more robust signatures of ejecta material in space is the low proton temperature [*Richardson and Cane*, 1995, and references therein], where by "low" we mean "substantially lower than the expected temperatures for the expanding solar wind." This is not the case here, and the heating evident in panel three is probably a result of the interaction. Note, however, that the proton beta (panel four) is generally below unity in the ejecta intervals, save for a $\sim$1-hour-long excursion at $\sim$1300 UT. The extremely high densities and fast speeds resulted in very elevated dynamic pressures being applied to the magnetosphere (panel four). Only sporadically do they approach values typical of 1 AU measurements ($\sim$2 nPa; see, for example, *Mühlbachler et al.* [2005, Figure 3]).

[19] Like the density, the trend in the total field profile is to decrease. Behind the shock it starts at exceptionally high values ($\sim$75 nT) just behind the shock and declines after that, while still remaining high throughout the ejecta intervals. We may note the extreme strength of the first, leading shock, one result of ejecta-ejecta interactions noted above: the density and the magnetic field are compressed by factor of $\sim$4 and $\sim$3, respectively; the Alfven Mach number of the shock is $\sim$6.0. Note that the field in the sheath region is mostly northward. There are two intervals of southward pointing magnetic field, one in each ejecta. We may note also that the leading ejecta has all the signatures of a magnetic cloud [*Burlaga et al.*, 1981]. (The electric field, panel five, will be discussed later).

[20] To summarize, two ejecta are seen by Wind in an advanced stage of coalescence. The interaction has caused a very strong shock in front of the leading ejecta, very compressed magnetic field strengths (with, in particular, large out-of-the-ecliptic components), and high plasma densities, and has heated the plasma, the latter indicated by the high values shown in the third panel of Figure 1, which are comparable to those expected from normal solar wind expansion.

4. *Dst* Measurements

[21] Figure 2 captures the main theme of the paper, a double-dip storm caused by two interacting ejecta. It shows in the top panels the magnetic field profile and that of its
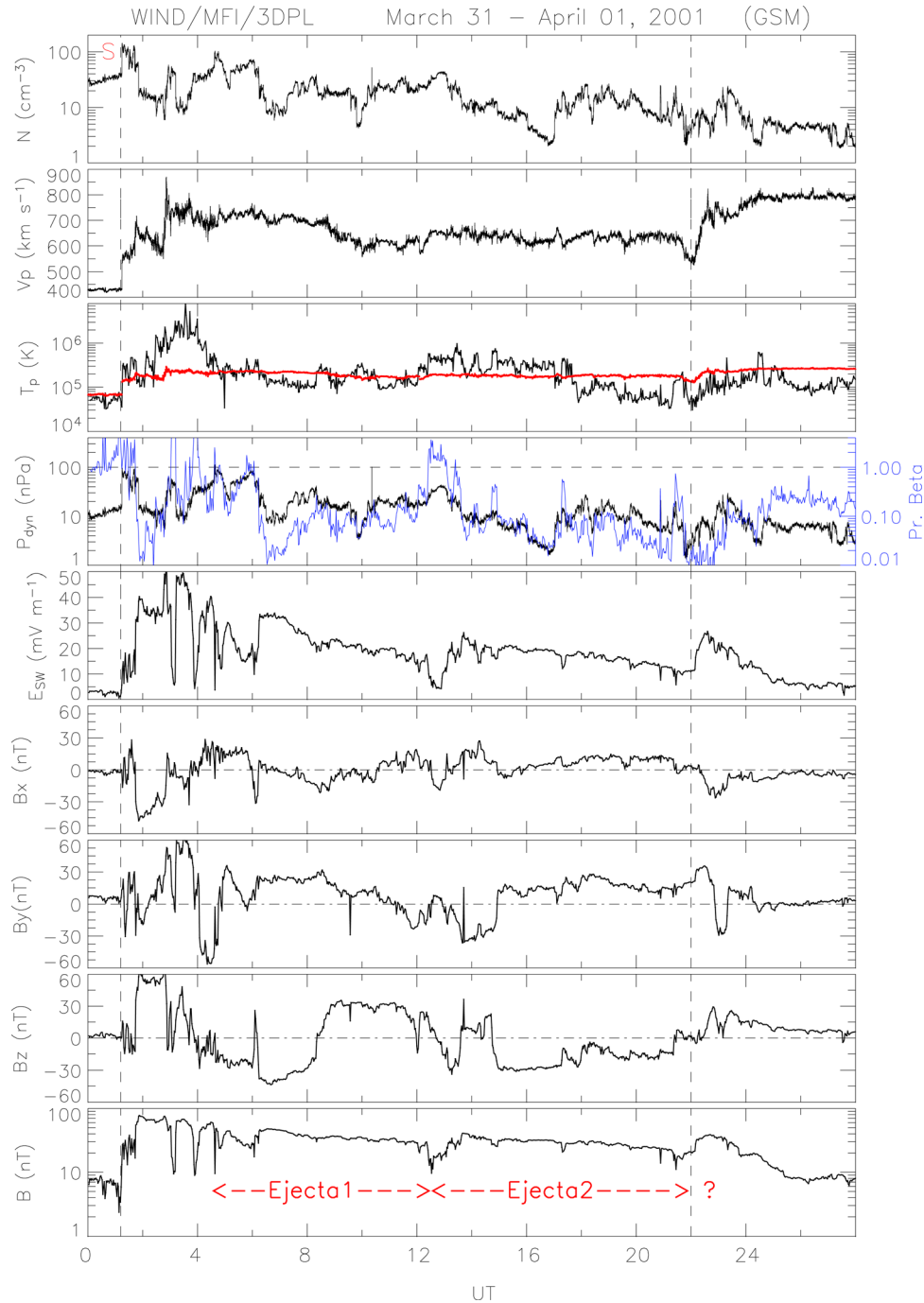
Figure 1. Magnetic field and plasma observations from spacecraft Wind for the period 0000 UT, 31 March, to 0400 UT, 1 April 2001, showing by dark traces the total density, proton bulk speed, temperature, and dynamic pressure, the solar wind electric field, the GSM components of the magnetic field and the total field. The red trace in panel three gives expected temperature from statistical correlations between solar wind proton temperature and speed. The blue trace is panel four is the proton plasma β (scale on the right). The vertical dashed lines indicate the arrival times of the shock ahead of the ejecta marger and the leading edge of a fast stream. The durations of the two ejecta are indicated in the bottom panel.

north-south component B_z for reference. The bottom panel shows by a black trace the *Dst* readings. The data are hourly averages. Two minima may be seen (arrowed), both below −250 nT ("great" storms), separated by ∼12 hours, and occurring during the successive passage of two $B_z < 0$ nT intervals, one in each ejecta. The first peak is bigger than the

second. Assuming Chapman-Ferraro scaling, i.e., that the magnetopause currents contribute to the depression of the horizontal component of the geomagnetic field in proportion to $\sqrt{P_{dyn}}$ with a (fixed) constant of proportionality = 15.8 in these units [*Burton et al.*, 1975], we obtain the disturbance shown by a red trace which, after forming hour
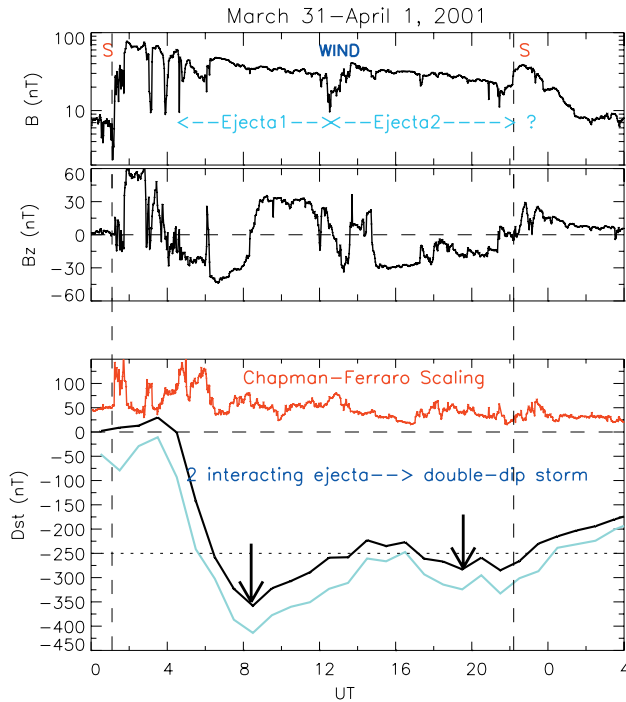
Figure 2. The double-dip great storm caused by the ejecta merger. The magnetic field profile in the top panel is reproduced for reference. In the bottom panel, the dark trace shows the *Dst* measurements over this period. The red trace gives the disturbance of the geomagnetic field at low latitudes due to magnetopause currents based on a constant proportionality with the square root of the solar wind dynamic pressure. The light blue trace shows the *Dst* measurements corrected for the the effects of these currents.

averages (light black trace), results in a correction to the *Dst* shown by a light blue trace. If this scaling were correct, it would alone cause a disturbance characteristic of a major-to-moderate storm. (Note, however, that estimates for the constant of proportionality vary by a factor of almost 3, from 13 to 34 [*Russell et al.*, 1992].) We return to this point in the Discussion.

5. High-Density Plasma Sheet in Relation to Solar Wind Densities

[22] We now take a closer look at the solar wind density. It will be shown in the next section that the massively dense, hot plasma sheet was the main factor in causing the great DD storm. We can ascribe this to a result of the merging of the two ejecta once we establish that it is of solar wind origin. This we do next.

[23] Figure 3 shows by the top black trace the solar wind density profile (called N_{sw} below) with its general exponential decreasing trend (roughly as $N \, [\mathrm{cm}^{-3}] = 60 \, e^{-0.1t[hr]}$). The colored data points below it are measurements of total ion densities above ~100 eV made at geostationary orbit by three LANL spacecraft in the nightside (1800–0600 MLT) plasma sheet (called N_{ps} below). A striking feature is the very high N_{ps} (up to ~10 cm^{-3}), and the generally similar temporal profiles of N_{sw} and N_{ps}, with a decreasing trend from ejecta 1 to ejecta 2. The second panel reproduces the

total field at Wind for reference. Visually, one can make out a good correlation between the two density profiles, suggesting a cause-effect relationship. Examining this further, we produce from these measurements a single-valued profile of N_{ps}. To do this, we retain all measurements where there is no overlap, and select the data acquired closest to local midnight where there is an overlap. The resulting profile is shown by the thin black trace in panel one where, for clarity, we have divided the values by 4.

[24] The bottom panel shows a scatterplot of N_{ps} versus N_{sw}. While there is scatter, the data are well fit by the relation $N_{ps} = 0.68 \, N_{sw}^{0.52}$ (R = 0.6; 658 data points). This result is good at better than the 99.9% confidence level. We may thus conclude that the hot dense plasma sheet on this day was of solar wind origin. This result is similar to that of *Borovsky et al.* [1998, Figure 1], only in this ejecta merger
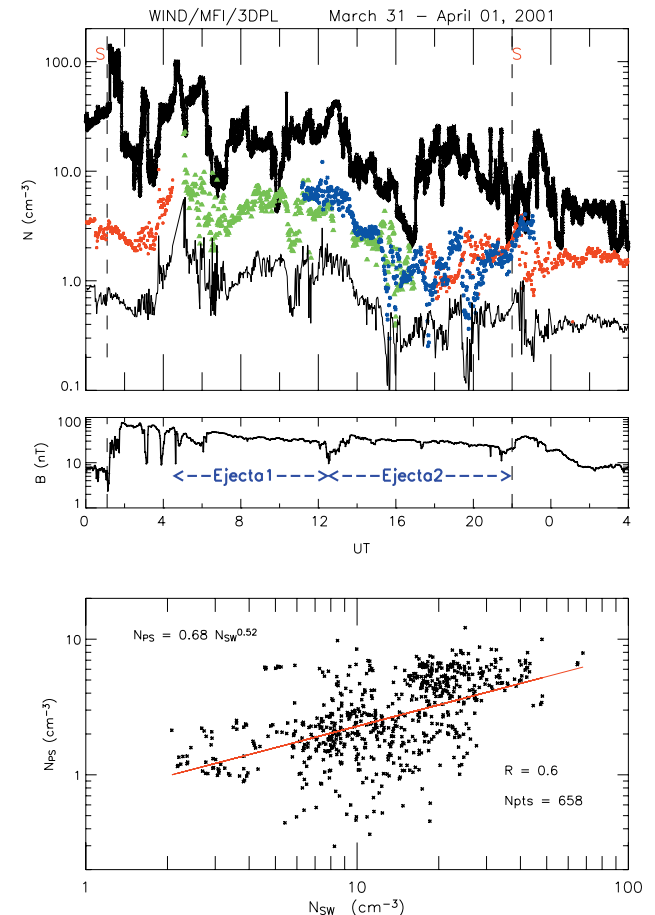

Figure 3. The solar wind and plasma sheet densities. The top panel shows by a thick black trace the solar wind density values. The colored data points give the readings of the nightside plasma sheet densities from three LANL geostationary spacecraft (shown in different color). The thin trace is a single-valued function made from these measurements as described in the text. It is divided by 4 for clarity of presentation. The middle panel shows the magnetic field for reference, with the ejecta intervals marked. The bottom panel a scatter plot of the two densities, and the correlation fit.

case, the dynamic range of N_{ps} is higher by a factor of 5 and superdense conditions last for many hours.

6. Modelling the Ring Current Behavior

[25] We now see what role, if any, the plasma sheet density had on the build-up of the ring current. In order to do this, we apply the global kinetic drift-loss model (see *Jordanova et al.* [1996, 2001a, 2001b, 2003] for more details). The dynamics of energetic charged particles of species l under the conditions of a time-varying magnetospheric electric field are studied by solving numerically the bounce-averaged kinetic equation for the phase space distribution function Q_l:

$$\frac{\partial Q_l}{\partial t} + \frac{1}{R_o^2}\frac{\partial}{\partial R_o}\left(R_o^2\left\langle\frac{dR_o}{dt}\right\rangle Q_l\right) + \frac{\partial}{\partial \phi}\left(\left\langle\frac{d\phi}{dt}\right\rangle Q_l\right)$$
$$+ \frac{1}{\sqrt{E}}\frac{\partial}{\partial E}\left(\sqrt{E}\left\langle\frac{dE}{dt}\right\rangle Q_l\right) \tag{1}$$

$$+ \frac{1}{h(\mu_o)\mu_o}\frac{\partial}{\partial \mu_o}\left(h(\mu_o)\mu_o\left\langle\frac{d\mu_o}{dt}\right\rangle Q_l\right) \tag{2}$$

$$= \left\langle\left(\frac{\partial Q_l}{\partial t}\right)_{ce}\right\rangle + \left\langle\left(\frac{\partial Q_l}{\partial t}\right)_{cc}\right\rangle + \left\langle\left(\frac{\partial Q_l}{\partial t}\right)_{wp}\right\rangle + \left\langle\left(\frac{\partial Q_l}{\partial t}\right)_{atm}\right\rangle \tag{3}$$

The left-hand side of the equation describes the adiabatic drift of ring current particles in time-dependent magnetospheric electric and magnetic fields. Below we shall use the semiempirical convection and corotation model of Volland-Stern [*Volland*, 1973; *Stern*, 1975], one of the most widely used inner magnetospheric electric field models. The right-hand side represents the loss terms, which are, in order of appearance, charge exchange with exospheric hydrogen (suffix *ce*), Coulomb collisions with thermal plasma (*cc*), wave-particle interactions (*wp*), and absorption of ring current particles at low altitude in the atmosphere (*atm*). The distributions of H^+, He^+, and O^+ ions are calculated as a function of time t, kinetic energy E from 100 eV to 500 keV, equatorial pitch angle α_o from 0° to 90°, where $\mu_o = \cos(\alpha_o)$, radial distance in the equatorial plane R_o from $2\,R_E$ to $6.5\,R_E$, and all magnetic local times (MLT) with geomagnetic longitude $\phi = 0$ at midnight. The magnetospheric plasma inflow on the nightside is modeled using energetic flux measurements made by the LANL spacecraft at geosynchronous orbit. The heavy ion content at the nightside boundary as a function of geomagnetic and solar activity is modeled after *Young et al.* [1982]. In the model, losses through the dayside magnetopause are also taken into account.

[26] Using this kinetic model, we simulated the temporal behavior of the ring current buildup during Earth passage of this ejecta merger. The strength of the ring current depends essentially on two factors: the convection electric field in which particles drift, and the seed population, i.e., the plasma sheet particles accelerated in from the nightside. Our aim is to see the effect of the very elevated plasma sheet
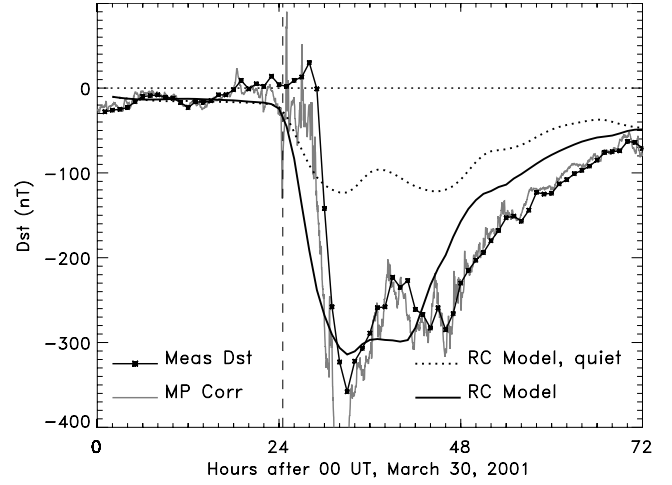

Figure 4. Results of the simulation of ring current buildup and decay. The data points joined by a solid line are the measured *Dst* values; the thin trace are the *Dst* values corrected for the effect of Chapman-Ferraro currents at the magnetopause; the dotted curve shows the result of the simulation when the nightside boundary condition assumes densities prior to the storm; the thick dark trace gives the results of the model when the nightside densities are determined by those measured by LANL spacecraft and shown in Figure 3.

density. Figure 4 shows the result of the calculations. The data points joined by a solid trace represents the measured *Dst*, uncorrected for magnetopause currents. The light trace reproduces the *Dst* after correcting them for the effect of magnetopause currents in the manner described in the previous section. The model is then run twice. First, it is run with quiet (prestorm) conditions in the plasma sheet. Thus this run takes into account only the changing electric field in which particles drift. This gives the dotted theoretical curve (marked "RC Model, quiet"). The ring current code is then run with the plasma sheet density updated according to LANL measurements, presented above. This yields the model curve shown by a solid line and marked "RC Model."

[27] The following points may be made: (1) Both model runs show a doubly peaked, major ring current enhancement due to the sequential arrival of $B_z < 0$ intervals in ejecta 1 and 2. (2) However, ignoring the enhanced plasma sheet densities yields in our model a *Dst* profile which greatly underestimates the data, by as much as a factor of ~2.5 near the *Dst* minima. (3) Including the enhanced plasma sheet density, on the other hand, gives a profile which is close to the measured one (*Dst* uncorrected for magnetopause currents), even if the predicted decay sets in sooner. It falls far short of predicting the *Dst* corrected for magnetopause currents using Chapman-Ferraro scaling. We return to the latter point in the discussion section when we consider recent literature on this issue. (4) An important point is that our modeling does not show any preconditioning ("priming") of the ring current. That is, irrespective of the prevailing energy of the ring current, a similar convection strength and duration applied subsequently would result in similar changes in Dst if the same boundary conditions are

applied. Specifically, the first storm does not "prime" the second.

7. Discussion and Conclusions

[28] We have examined a case of a two-step geomagnetic storm where the two peaks in the Dst index, a measure of the energy content of the ring current, were two negative B_z intervals in two ejecta in an advanced stage of coalescence. The interaction occurred when two coronal mass ejections emitted by the Sun collided en route to Earth. The Earth "senses" the presence of the second ejection by a reactivation of ring current when the first burst of activity had started to subside. In this case the major factor determining the severity of both storms was the enhanced plasma sheet density, with a temporally decreasing trend. Both N_{sw} and N_{ps} show extraordinarily large values. Compared to the large statistical study undertaken by *Borovsky et al.* [1998], the observations extend the range of superdense (density >1 cm^{-3}) plasma sheets by a factor of ~5. The solar wind densities are several standard deviation away from those measured in isolated ejecta near the last solar minimum [*Lepping et al.*, 2003]. A good correlation between the solar wind and the plasma sheet densities was found, suggesting strongly that the IP origin of this hot, dense plasma sheet was the solar wind. The ring current behavior was modeled well only when the high plasma sheet densities were included as nightside boundary condition, and thus the exact extent of ring current build-up is a direct consequence of the ejecta-ejecta interaction because compression of the plasma in the leading ejecta was a necessary concomitant of this interaction. Note that the coalescence was not complete. While the shock ahead of the trailing ejecta had dissipated away and transferred its momentum and that of its postshock flow to the leading ejecta [*Farrugia and Berdichevsky*, 2004], there is yet a vestige of a boundary between the interacting ejecta, when the proton plasma β rises briefly above unity (Figure 1) and a Forbush decrease is still present (not shown).

[29] The example is a demonstration of a hitherto little recognized mechanism by which DD storms may arise, and one quite distinct from the traditional "shock-driver gas" mechanism [*Tsurutani et al.*, 1988] invoked as IP origin of DD storms [*Kamide et al.*, 1998, and references therein]. In particular, in DD storms where the first Dst min is more pronounced than the second; they constituted 8.5% of all major ($Dst < -100$ nT) storms in the survey of *Kamide et al.* [1998]; we expect ejecta mergers to play a leading role. Yet, as discussed further below, under certain circumstances the two IP origins may be superposed, complementing each other.

[30] The importance of this new mechanism to space weather studies clearly depends among other things on how often it happens. The short answer is that this question has yet to be pursued in a large, systematic survey. However, there is circumstantial evidence to suggest that it may be quite frequent. In a recent work, *Farrugia et al.* [2006] surveyed large magnetospheric disturbances, as measured by the Dst index, and the corresponding IP structures, over the 9-year period 1996–2003. To define "large," they computed in the *Perreault and Akasofu* [1978] "ε" formulation the powering of the magnetosphere by the solar wind

and the energy extracted by the magnetosphere from the solar wind (time integral of ε). This formulation was chosen because parameter ε can be computed from IP parameters and hence, in principle, large disturbances can be predicted. They found the energy and power per unit area extracted from the solar wind to hardly ever exceed 12 J m^{-2} (computed over 3 days) and 0.4 mW m^{-2} (computed over 3 hours), respectively. Those which did were labeled "large events." In agreement with other studies (see section 1), the IP configurations responsible for many of these large events were either magnetic clouds [*Burlaga et al.*, 1981] or ejecta [*Gosling*, 1990; *Gosling et al.*, 1990, 1991]. Importantly, a significant number of the strongest storms were elicited by ejecta interacting with each other.

[31] Near solar activity maximum many instances have been recorded where a large number of coronal mass ejections were emitted in quick succession from the Sun directed toward Earth, increasing the likelihood of ejecta-ejecta interactions [*Gopalswamy et al.*, 2001, 2002]. Thus it may be supposed that this mechanism is most relevant during the maximum phase of the solar cycle.

[32] An interesting point is that the Dst measured on 31 March 2001, is reproduced well by the simulation, but falls far short of the Dst when a Chapman-Ferraro correction is included for the effect of magnetopause currents (i.e., a fixed constant of proportionality relating the ground magnetic disturbance to the square root of the solar wind dynamic pressure). Carrying out an extensive analysis of the *Burton et al.* [1975] equation relating the rate of change of the Dst with the solar wind electric field, E_{sw}, and dynamic pressure, *O'Brien and McPherron* [2000, 2002] and *McPherron and O'Brien* [2001] were the first to show that this constant of proportionality varies strongly with E_{sw}, decreasing by a large factor as E_{sw} increases from a 0 to 18 mV m^{-1}.

[33] As has been discussed by *Russell et al.* [2001] and *Siscoe et al.* [2002, 2005], under a strong E_{sw}, the magnetosphere exhibits nonlinear behavior. In particular, the cross-polar cap potential saturates, i.e., becomes independent of E_{sw}. The E_{sw} in the event we studied is intense enough for these saturation phenomena to develop. Studying dayside magnetosphere erosion over the time period 1996–2004, using the depression of the geostationary field as monitor [*Sibeck*, 1994], *Mühlbachler et al.* [2005] found that saturation appears at $E_{sw} \approx 6$ mV m^{-1}. This value is exceeded in our case (see Figure 1, panel five). We may thus expect that in our event saturation has occurred. Indeed, saturation of cross-polar cap potential for the second ejecta on 31 March 2001 was shown directly using DMSP measurements by *Hairston et al.* [2003], who compared them with the theoretical formulation of the Hill-Siscoe transpolar potential saturation model given by *Siscoe et al.* [2002].

[34] Under high solar wind electric fields, the role of the Chapman-Ferraro current in standing off the solar wind is taken over by the Region 1 current [*Hill*, 1976; *Siscoe et al.*, 2002]. Elaborating this point further, *Siscoe et al.* [2005] find that the scaling factor may then become energy-dependent and decrease, though the issue as to how this is achieved is still under debate. If that is the case, the lack of agreement of model predictions with the corrected Dst on 31 March 2001, would stem mainly from the fact that
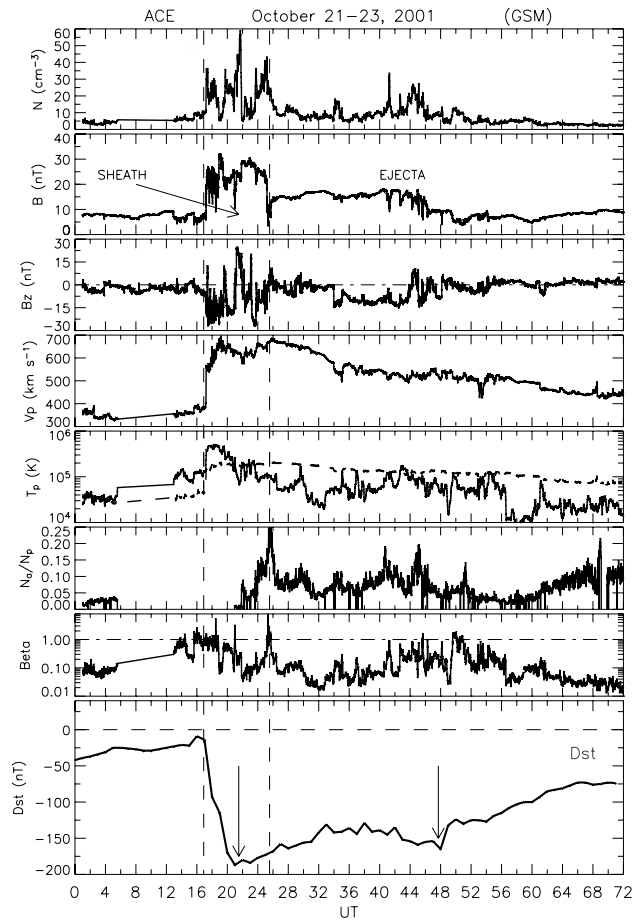
Figure 5. ACE observations during the passage of the ejecta merger on 21–23 October 2001. From top to bottom are shown the proton density, total field strength and its GSM B_z component, the bulk speed and temperature, the α particle-to-proton number density ratio, and the proton plasma beta. The two vertical dashed guidelines indicate the times of the shock and the estimated front edge of the ejecta. The dashed trace in the fifth panel shows the expected temperature for normal solar wind expansion. The bottom panel shows *Dst* readings, with two minima during the sheath and ejecta passages, respectively.

during strong disturbances CF scaling tends to overestimate the correction to *Dst*.

[35] A recent work bearing directly on this problem is that of *Feldstein et al.* [2005]. They calculated the distortions of the geomagnetic field in a self-consistent version of their time-dependent magnetospheric model. They find that around storm maximum, the disturbance of the Earth's field by the Chapman-Ferraro current is almost equal and opposite to that resulting from the tail current and thus the effects of the two current systems nearly cancel.

[36] It is not being claimed, of course, that all ejecta-ejecta interactions cause DD storms or that all DD storms are due to ejecta-ejecta interactions. An essential requirement is the presence of a $B_z < 0$ nT interval in each of the participating ejecta, which is needed to activate the magnetosphere through reconnection. Further, as mentioned earlier, ejecta-ejecta interactions may sometimes act as a

complementary mechanism to the "sheath-driver gas" mechanism. A possible illustration of this point may be the multiple ejecta which reached Earth on 21–25 October 2001. To illustrate this point, we show in Figure 5 select interplanetary parameters from the ACE spacecraft for part of this long ejecta passage, 21–23 October 2001: the proton density, magnetic field strength, the GSM B_Z component of the field, the proton bulk speed, temperature, the proton-to-α particle number density ratio, and the proton plasma β. On the basis of the generally strong fields, the high α/proton number density ratio, low (<1) proton plasma β, and the declining *V*-profile after the shock, which continue until ~0900 UT, 25 October when another shock is seen advancing into this complex (not shown), we may conclude that this is a compound stream [*Burlaga et al.*, 1987] formed by the interaction of at least two ejecta. The profile of the measured *Dst* index in the bottom panel shows the presence of a DD storm. Without doubt, the first, and strongest, *Dst* peak occurs during the passage of the sheath, while the ejecta merger gave rise to the second *Dst* minimum. (There were no further intervals of negative B_z, and the *Dst* continued to recover after this.) So the compression of preexisting $B_z < 0$ fields by the shock was the cause of the major *Dst* peak. With a compression ratio of *N* and *B* $\approx$ 3, the leading shock is a moderately strong shock. Now, the compression of pre-existing $B_z < 0$ fields depends on the strength of this shock. In so far as ejecta interactions tend to strengthen the leading shock, it seems to us reasonable to suppose that the shock may have derived part of its strength, and hence part of its ability to compress upstream fields, from the interaction of the ejecta. It is thus possible that, by enhancing the strength of the shock ahead of the ejecta merger, the interaction intensified the effect of the shock. Thus the strength of the first storm may be considered as being caused by a superposition of two triggers.

References

Berdichevsky, D. B., C. J. Farrugia, R. P. Lepping, A. B. Galvin, R. Schwenn, D. V. Reames, K. W. Ogilvie, and M. L. Kaiser (2003), Solar-heliospheric-magnetospheric observations on March 23–April 26, 2001: Similarities to observations in April 1979, in *Solar Wind Ten*, edited by M. Velli, R. Bruno, and F. Malara, *AIP Conf. Proc.*, *679*, 699.

Borovsky, J. E., M. F. Thomsen, and R. C. Elphic (1998), The driving of the plasma sheet by the solar wind, *J. Geophys. Res.*, *103*, 17,617.

Burlaga, L. F., E. Sittler, F. Mariani, and R. Schwenn (1981), Magnetic loop behind an interplanetary shock: Voyager, Helios and IMP 8 observations, *J. Geophys. Res.*, *86*, 6673.

Burlaga, L. F., K. W. Behannon, and L. W. Klein (1987), Compound streams, magnetic clouds and major geomagnetic storms, *J. Geophys. Res.*, *92*, 5725.

Burlaga, L. F., R. P. Lepping, and J. Jones (1990), Global configuration of a magnetic cloud, in *Physics of Magnetic Flux Ropes*, *Geophys. Monogr. Ser.*, vol. 58, edited by C. T. Russell, E. R. Priest, and L. C. Lee, p. 373, AGU, Washington, D. C.

Burlaga, L. F., R. M. Skoug, C. W. Smith, D. F. Webb, T. H. Zurbuchen, and A. Reinard (2001), Fast ejecta during the ascending phase of solar cycle 23: ACE observations, 1998–1999, *J. Geophys. Res.*, *106*, 20,957.

Burlaga, L. F., S. P. Plunkett, and P.-C. St. Cyr (2002), Successive CMEs and complex ejecta, *J. Geophys. Res.*, *107*(A10), 1266, doi:10.1029/ 2001JA000255.

Burton, R. K., R. L. McPherron, and C. T. Russell (1975), An empirical relationship between interplanetary conditions and *Dst*, *J. Geophys. Res.*, *80*, 4204.

Cane, H. V., and I. G. Richardson (2003), Interplanetary coronal mass ejections in the near-Earth solar wind during 1996–2002, *J. Geophys. Res.*, *108*(A4), 1156, doi:10.1029/2002JA009817.

Crooker, N. U., G. L. Siscoe, C. T. Russell, and E. J. Smith (1982), Factors controlling degree of corelation between ISEE 1 and ISEE 3 interplanetary magnetic field measurements, *J. Geophys. Res.*, *97*, 2224.

Daglis, I. A., J. U. Kozyra, Y. Kamide, D. Vassiliades, A. S. Sharma, M. W. Liemohn, W. D. Gonzalez, B. T. Tsurutani, and G. Lu (2003), Intense space storms: Critical issues and open disputes, *J. Geophys. Res.*, *108*(A5), 1208, doi:10.1029/2002JA009722.

Farrugia, C. J., M. P. Freeman, L. F. Burlaga, R. P. Lepping, and K. Takahashi (1993a), The Earth's magnetosphere under continued forcing: Substorm activity during the passage of an interplanetary magnetic cloud, *J. Geophys. Res.*, *98*, 76571993.

Farrugia, C. J., L. F. Burlaga, V. A. Osherovich, I. G. Richardson, M. P. Freeman, R. P. Lepping, and A. J. Lazarus (1993b), A study of an expanding interplanetary magnetic cloud and its interaction with the Earth's magnetosphere: The interplanetary aspect, *J. Geophys. Res.*, *98*, 7621.

Farrugia, C. J., I. G. Richardson, L. F. Burlaga, R. P. Lepping, and V. A. Osherovich (1993c), Simultaneous observations of solar MeV particles in a magnetic cloud and in the Earth's northern tail lobe: Implications for the global field line topology of magnetic clouds and entry of solar particles into the tail lobe during cloud passage, *J. Geophys. Res.*, *98*, 15,497.

Farrugia, C. J., L. F. Burlaga, and R. P. Lepping (1997), Magnetic clouds and the quiet-storm effect at Earth, in *Magnetic Storms*, *Geophys. Monogr. Ser.*, vol. 98, edited by B. T. Tsurutani et al., p. 91, AGU, Washington, D. C.

Farrugia, C. J., et al. (1998), Geoeffectiveness of three Wind magnetic clouds: A comparative study, *J. Geophys. Res.*, *103*, 17,261.

Farrugia, C. J., and D. B. Berdichevsky (2004), Evolutionary signatures in complex ejecta and their driven shocks, *Ann. Geophys.*, *22*, 3679–3698.

Farrugia, C. J., et al. (2005a), Interplanetary coronal mass ejection and ambient interplanetary magnetic field correlations during the Sun-Earth connection events of October–November 2003, *J. Geophys. Res.*, *110*, A09S13, doi:10.1029/2004JA010968.

Farrugia, C. J., et al. (2005b), Cross-correlation of interplanetary parameters for large (∼450 R_E) separation: Dependence on interplanetary structure, in *Solar Wind Eleven*, edited by B. Fleck and T. H. Zurbuchen, *Eur. Space Agency Spec. Publ.*, ESA SP-592, 719.

Farrugia, C. J., H. Matsui, H. Kucharek, V. K. Jordanova, R. B. Torbert, K. W. Ogilvie, D. B. Berdichevsky, C. W. Smith, and R. Skoug (2006), Survey of intense Sun-Earth connection events (1995–2003), *Adv. Space. Res.*, in press.

Feldstein, Y. I., et al. (2005), Self-consistent modeling of the large-scale distortions in the geomagnetic field during the 24–27 September 1998 major magnetic storm, *J. Geophys. Res.*, *110*, A11214, doi:10.1029/2004JA010584.

Freeman, M. P., C. J. Farrugia, L. F. Burlaga, M. R. Hairston, M. Greenspan, J. M. Ruohoniemi, and R. P. Lepping (1993), The interaction of a magnetic cloud with the Earth: Ionospheric convection in the northern and southern hemispheres for a wide range of quasi-steady interplanetary magnetic field conditions, *J. Geophys. Res.*, *98*, 7633.

Gibson, S. E., and B. C. Low (1998), A time-dependent three-dimensional magnetohydrodynamic model of the coronal mass ejection, *Astrophys. J.*, *493*, 460.

Gonzalez, W. D., and B. T. Tsurutani (1987), Criteria of interplanetary parameters causing intense magnetic storms (*Dst* < −100 nT), *Planet. Space Sci.*, *35*, 1101.

Gonzalez, W. D., B. T. Tsurutani, A. L. Clua de Gonzalez, F. Tang, E. J. Smith, and S.-I. Akasofu (1989), Solar wind-magnetosphere coupling during intense geomagnetic storms (1978–1979), *J. Geophys. Res.*, *94*, 8835.

Gopalswamy, N., S. Yashiro, M. L. Kaiser, R. A. Howard, and J.-L. Bougeret (2001), Radio signatures of coronal mass ejection interaction: Coronal mass ejection cannibalism?, *Astrophy. J.*, *548*, L91.

Gopalsamy, N., S. Yashiro, M. L. Kaiser, R. A. Howard, and J.-L. Bougeret (2002), Interplanetary radio emission due to interaction between two coronal mass ejections, *Geophys. Res. Lett.*, *29*(8), 1265, doi:10.1029/2001GL013606.

Gosling, J. T. (1990), Coronal mass ejections and flux ropes in interplanetary space, in *Physics of Magnetic Flux Ropes*, *Geophys. Monogr. Ser.*, vol. 58, edited by C. T. Russell, E. R. Priest, and L. C. Lee, p. 343, AGU, Washington, D. C.

Gosling, J. T. (1993), Coronal mass ejections: The link between solar and geomagnetic activity, *Phys. Fluids, B*, *5*(7), 2638.

Gosling, J. T., D. N. Baker, S. J. Bame, W. C. Feldman, R. D. Zwickl, and E. J. Smith (1987), Bidirectional solar wind electron heat flux events, *J. Geophys. Res.*, *92*, 8519.

Gosling, J. T., S. J. Bame, D. J. McComas, and J. L. Phillips (1990), Coronal mass ejections and large geomagnetic storms, *Geophys. Res. Lett.*, *17*, 901.

Gosling, J. T., D. J. McComas, J. L. Phillips, and S. J. Bame (1991), Geomagnetic activity associated with Earth-passage of interplanetary shock disturbances and coronal mass ejections, *J. Geophys. Res.*, *96*, 7831.

Hairston, M. R., T. W. Hill, and R. A. Heelis (2003), Observed saturation of the ionospheric polar cap potential during the 31 March 2001 storm, *Geophys. Res. Lett.*, *30*(6), 1325, doi:10.1029/2002GL015894.

Hill, T. W. (1976), Mercury and Mars: The role of ionopsheric conductivity in the acceleration of magnetospheric particles, *Geophys. Res. Lett.*, *3*, 429.

Huang, C.-S., J. C. Foster, G. D. Reves, G. Le, H. U. Frey, C. J. Pollock, and J.-M. Jahn (2003a), Periodic magnetospheric substorms: Multiple space-based and ground-based intrumental observations, *J. Geophys. Res.*, *108*(A11), 1411, doi:10.1029/2003JA009992.

Huang, C.-S., G. D. Reves, J. E. Borovsky, R. M. Skoug, Z. Y. Pu, and G. Le (2003b), Periodic magnetospheric substorms and their relationship with solar wind variations, *J. Geophys. Res.*, *108*(A11), 1255, doi:10.1029/2002JA009704.

Jordanova, V. K., L. M. Kistler, J. U. Kozyra, G. V. Khazanov, and A. F. Nagy (1996), Collisional losses of ring current ions, *J. Geophys. Res.*, *101*, 111.

Jordanova, V. K., C. J. Farrugia, J. F. Fennell, and J. D. Scudder (2001a), Ground disturbances of the ring, magnetopause, and tail currents on the day the solar wind almost disappeared, *J. Geophys. Res.*, *106*, 25,529.

Jordanova, V. K., R. M. Thorne, C. J. Farrugia, J. F. Fennell, M. F. Thomsen, G. D. Reeves, and D. J. McComas (2001b), Ring current dynamics during the July 14–18, 2000, storm, *Solar Phys.*, *204*, 361.

Jordanova, V. K., L. M. Kistler, M. F. Thomsen, and C. G. Mouikis (2003), Effects of plasam sheet variability on the fast initial ring current decay, *Geophys. Res. Lett.*, *30*(6), 1311, doi:10.1029/2002JA016576.

Kamide, Y., N. Yokoyama, W. Gonzalez, B. T. Tsurutani, I. A. Daglis, A. Brekke, and S. Masuda (1998), Two-step development of geomagnetic storms, *J. Geophys. Res.*, *103*, 6917.

Lepping, R. P., et al. (1995), The Wind Magnetic Field Investigation, *Space Sci. Rev.*, *71*, 207.

Lepping, R. P., D. B. Berdichevsky, A. Szabo, C. Arqueros, and A. J. Lazarus (2003), Profile of an average magnetic cloud at 1 AU for the quiet solar phase: Wind Observations, *Solar Phys.*, *212*, 425.

Lin, R. P., et al. (1995), A Three-Dimensional Plasma and Energetic Particle Investigation for the Wind spacecraft, *Space Sci. Rev.*, *71*, 125.

Lopez, R. E. (1987), Solar cycle invariance in solar wind proton temperature relationships, *J. Geophys. Res.*, *92*, 11,187.

Lugaz, N., W. B. Manchester, and T. I. Gombosi (2005), Numerical simulation of the interaction of two coronal mass ejections from Sun to Earth, *Astrophys. J.*, *634*, 651.

McPherron, R. L., and T. P. O'Brien (2001), Predicting geomagnetic activity: The *Dst* index, in *Space Weather*, *Geophys. Monogr. Ser.*, vol. 125, edited by P. Song, H. Singer, and G. Siscoe, p. 339, AGU, Washington, D. C.

Mühlbachler, S., C. J. Farrugia, J. Raeder, H. K. Biernat, and R. B. Torbert (2005), A statistical investigation of dayside magnetosphere erosion showing saturation of response, *J. Geophys. Res.*, *110*, A11207, doi:10.1029/2005JA011177.

Neugebauer, M., and R. Goldstein (1997), Particle and field signatures of coronal mass ejections in the solar wind, in *Coronal Mass Ejections*, *Geophys. Monogr. Ser.*, vol. 99, p. 245, edited by N. Crooker, J. A. Joselyn, and J. Feynman, AGU, Washington, D. C.

O'Brien, T. P., and R. L. McPherron (2000), An empirical phase space analysis of ring current dynamics: Solar wind control of injection and decay, *J. Geophys. Res.*, *105*, 7707.

O'Brien, T. P., and R. L. McPherron (2002), Seasonal and diurnal variation of *Dst* dynamics, *J. Geophys. Res.*, *107*(11), 1341, doi:10.1029/2002JA009435.

Odstrcil, D., M. Vandas, V. J. Pizzo, and P. MacNeice (2003), Numerical simulation of interacting magnetic flux ropes, in *Solar Wind Ten*, edited by M. Velli, R. Bruni, and F. Malara, *AIP Conf. Proc.*, *679*, 758.

Ogilvie, K. W. O., et al. (1995), A Comprehensive Plasma Instrument for the Wind Spacecraft, *Space Sci. Rev.*, *71*, 55.

Perreault, P., and S.-I. Akasofu (1978), A study of geomagnetic storms, *Geophys. J. R. Astron. Soc.*, *54*, 547.

Richardson, I. G., and H. V. Cane (1995), Regions of abnormally low proton temperature in the solar wind (1965–1991) and their association with ejecta, *J. Geophys. Res.*, *100*, 23,397.

Richardson, J. D., and K. I. Paularena (2001), Plasma and magnetic field correlations in the solar wind, *J. Geophys. Res.*, *106*, 239.

Russell, C. T., M. Ginskey, S. Petrinec, and G. Le (1992), The effect of solar wind dynamic pressure on low and mid-latitude magnetic records, *Geophys. Res. Lett.*, *19*, 1227.

Russell, C. T., J. G. Luhmann, and G. Lu (2001), Nonlinear response of the polar ionosphere to large values of the interplanetary electric field, *J. Geophys. Res.*, *106*, 18,495.

Sibeck, D. G. (1994), Signatures of flux erosion from the dayside magnetosphere, *J. Geophys. Res.*, *99*, 8513.

Siscoe, G. L., et al. (2002), Hill model of transpolar potential saturation: Comparison with MHD simulations, *J. Geophys. Res.*, *107*(A7), 1094, doi:10.1029/2001JA000152.

Siscoe, G. L., R. L. McPherron, and V. K. Jordanova (2005), Diminsihed contribution of ram pressure to *Dst* during magnetic storms, *J. Geophys. Res.*, *110*, A12227, doi:10.1029/2005JA011120.

Stern, D. P. (1975), The motion of a proton in the equatorial magnetosphere, *J. Geophys. Res.*, *80*, 595.

Tsurutani, B. T., W. D. Gonzalez, F. Tang, S. I. Akasofu, and E. J. Smith (1988), Origin of interplanetary southward magnetic fields responsible for major magnetic storms near solar maximum (1978–1979), *J. Geophys. Res.*, *93*, 8519.

Tsurutani, B. T., W. D. Gonzalez, F. Tang, and Y. T. Lee (1992), Great magnetic storms, *Geophys. Res. Lett.*, *19*, 73.

Volland, H. (1973), A semiempirical model of large-scale magnetospheric electric fields, *J. Geophys. Res.*, *78*, 171.

Wang, Y. M., P. Z. Ye, and S. Wang (2003), Multiple magnetic clouds: Several examples during March–April, 2001, *J. Geophys. Res.*, *108*(A10), 1370, doi:10.1029/2003JA009850.

Young, D. T., H. Balsiger, and J. Geiss (1982), Correlations of magnetospheric ion composition with geomagnetic and solar activity, *J. Geophys. Res.*, *87*, 9077.

Zhang, G., and L. F. Burlaga (1987), Magnetic clouds, geomagnetic disturbances and cosmic ray decreases, *J. Geophys. Res.*, *93*, 2511.

Zwickl, R. D., J. R. Asbridge, S. J. Bame, W. C. Feldman, J. T. Gosling, and E.J. Smith (1983), Plasma properties of driver gas following interplanetary shocks observed by ISEE-3, in *Solar Wind Five*, edited by M. Neugebauer, *NASA Conf. Proc.*, *CP-2280*, 711.

————————————

S. W. H. Cowley, Department of Physics and Astronomy, University of Leicester, University Road, Leicester LE1 7RH, UK. (swhc1@ion.le.ac.uk)

C. J. Farrugia, Space Science Center and Department of Physics, University of New Hampshire, Morse Hall, Room 414, 39 College Road, Durham, NH 03824-3525, USA. (charlie.farrugia@unh.edu)

G. Lu, High Altitude Observatory, National Center for Atmospheric Research, 3080 Center Green, Boulder, CO 80301, USA. (ganglu@hao.ucar.edu)

K. W. Ogilvie, NASA Goddard Space Flight Center, MC 692, Greenbelt, MD 20771, USA. (keith.w.ogilvie@nasa.gov)

V. K. Jordanova and M. F. Thomsen, Los Alamos National Laboratory, P. O. Box 1663, MS D466, Los Alamos, NM 87545, USA. (mthomsen@lanl.gov)